Neurotherapeutics (2012) 9:185–198
DOI 10.1007/s13311-011-0072-y

ORIGINAL ARTICLE

C3 Peptide Promotes Axonal Regeneration and Functional Motor Recovery after Peripheral Nerve Injury

Stefanie C. Huelsenbeck · Astrid Rohrbeck · Annelie Handreck · Gesa Hellmich · Eghlima Kiaei · Irene Roettinger · Claudia Grothe · Ingo Just · Kirsten Haastert-Talini

Published online: 25 August 2011

Abstract Peripheral nerve injuries are frequently seen in trauma patients and due to delayed nerve repair, lifelong disabilities often follow this type of injury. Innovative therapies are needed to facilitate and expedite peripheral nerve regeneration. The purpose of this study was to determine the effects of a 1-time topical application of a 26-amino-acid fragment ($C3^{156-181}$), derived from the *Clostridium botulinum* C3-exoenzyme, on peripheral nerve regeneration in 2 models of nerve injury and repair in adult rats. After sciatic nerve crush, different dosages of $C3^{156-181}$ dissolved in buffer or reference solutions (nerve growth factor or $C3^{bot}$-wild-type protein) or vehicle-only were injected through an epineurial opening into the lesion sites. After 10-mm nerve autotransplantation, either 8.0 nmol/kg $C3^{156-181}$ or vehicle were injected into the proximal and distal suture sites. For a period of 3 to 10 postoperative weeks, $C3^{156-181}$-treated animals showed a faster motor recovery than control animals. After crush injury, axonal outgrowth and elongation were activated and consequently resulted in faster motor recovery. The nerve autotransplantation model further elucidated that $C3^{156-181}$ treatment accounts for better axonal elongation into motor targets and reduced axonal sprouting, which are followed by enhanced axonal maturation and better axonal functionality. The effects of $C3^{156-181}$ are likely caused by a nonenzymatic down-regulation of active RhoA. Our results indicate the potential of $C3^{156-181}$ as a therapeutic agent for the topical treatment of peripheral nerve repair sites.

Keywords Sciatic nerve · Crush injury · 10-mm nerve gap · Autotransplantation · $C3^{156-181}$ peptide

Electronic supplementary material The online version of this article (doi:10.1007/s13311-011-0072-y) contains supplementary material, which is available to authorized users.

S. C. Huelsenbeck · A. Rohrbeck · I. Just
Hannover Medical School, Institute of Toxicology,
Hannover 30625 Germany

A. Handreck · G. Hellmich · E. Kiaei · I. Roettinger · C. Grothe · K. Haastert-Talini (✉)
Hannover Medical School, Institute of Neuroanatomy,
Hannover 30625 Germany
e-mail: Haastert.kirsten@mh-hannover.de

C. Grothe · K. Haastert-Talini
Center for Systems Neuroscience (ZSN),
Hannover, Germany

Present Address:
S. C. Huelsenbeck
Institute of Toxicology, University Medical Center
of the Johannes-Gutenberg-University Mainz,
Mainz 55131 Germany

Introduction

Peripheral nerve injuries affect 2.8% of trauma patients who often acquire lifelong disability [1]. The annual incidence of peripheral nerve injuries ranges from 13.9 in 100,000 inhabitants in Sweden [2] to 300,000 cases in Europe [3]. Regeneration of peripheral nerves after different types of injury is generally possible, but the degree of recovery of peripheral sensory and motor functions depends on the type of the lesion and the distance across which the severed axons must grow to re-innervate their distal targets [4, 5]. Insufficient functional recovery is presumably related to at first variable time points after nerve transection at which axonal sprouts begin to elongate ("staggered outgrowth") [6] and at second to re-innervation of inappropriate pathways [7]. After nerve crush injury, the continuity of the endoneurial tubes is preserved and usually allows high degrees of functional recovery [8]. Neurosurgical intervention is needed, when complete nerve transection or even gaps between separated

nerve stumps occur [9]. Transplantation of less important sensory nerve trunks is the clinical gold standard to overcome larger nerve gaps (20 mm in humans), but this technique also cannot ensure the recovery of normal sensorimotor functions in adult patients [10]. The results achieved with nerve autografting are variable, ranging from extremely poor [11], including paresthesia and uncoordinated muscle contraction [12], to very good [13]. Innovative concepts for therapeutic interventions, therefore, are needed [4].

One concept is the transplantation of glia cells because the success of nerve autotransplantation is mainly attributed to the presence of Schwann cells [4]. The beneficial effects of transplanted glia cells (Schwann cells and olfactory ensheathing cells) have been clearly demonstrated in several animal studies [14–17]. Donor Schwann cells do integrate with the host tissue and contribute to the myelination of regenerated axons and the formation of adequately reconstituted nodes of Ranvier et al. [15]. Nearly the same behavior was demonstrated for transplanted olfactory ensheathing cells, which also accounted for increased functional recovery [14]. However, extensive studies also demonstrate that transplantation of primary or genetically modified glia cells alone are not sufficient to guarantee complete recovery from severe peripheral nerve injuries [18–21]. Therefore, other innovative stand-alone or combined therapeutic approaches are of high interest.

The administration of therapeutic agents from bacterial origin could be such an innovative approach. Botulinum neurotoxin, for example, has become a valid tool in the treatment of neurological diseases related to different types of spasm [22]. Clostridial C3 exoenzyme has been demonstrated to promote axonal repair mechanisms after spinal cord injury [23] and it has recently been demonstrated that intrathecal treatment with a 29-amino-acid fragment ($C3^{154-182}$) derived from full-length *Clostridium botulinum* C3 exoenzyme ($C3^{bot}$), improves axonal and functional recovery after spinal cord contusion or hemisection injury [24].

Here we tested the effect of the shortest active peptide derived from $C3^{bot}$, the 26-amino-acid fragment, $C3^{156-181}$, on peripheral nerve regeneration. We used established paradigms of sciatic nerve injury and repair in adult rats [18, 21, 25], which enable functional, as well as histomorphological evaluation of regeneration. Our results indicate that $C3^{156-181}$ promotes axonal elongation, maturation, and functional motor recovery after peripheral nerve injury and repair.

Methods

$C3^{bot}$ Purification and $C3^{156-181}$ Synthesis

$C3^{156-181}$ was synthesized at IPF PharmaCeuticals GmbH (Hannover, Germany). The lyophilized peptide was reconstituted in phosphate buffered saline (PBS) (137 mM NaCl, 3 mM KCl, 6.6 mM Na_2HPO_4,1.5 mM KH_2PO_4, pH 7.5), sterile filtered (0.22 μm), and used for the experiments as indicated as follows.

$C3^{bot}$ was expressed as recombinant GST-fusion protein expressed in *Escherichia coli* using the pGEX-2T vector system and purified by affinity chromatography using glutathione-sepharose. $C3^{bot}$ was mobilized from the glutathione-sepharose by thrombin digest.

Experimental Design

Animals and Surgical Procedures

Animal experiments were conducted in accordance with the German law on the protection of animals (approved by the Animal Care Committee of Lower-Saxony: 33H-42502-08/1564+09/1641).

Adult female Sprague-Dawley rats (200 g, 8 weeks [Charles River, Sulzfeld, Germany]) were housed in groups of 4 rats in Makrolon type IV cages (Ebeco, Castrop-Rauxel, Germany) under standard conditions (room temperature 22±2°C, humidity 55±5%, light/dark-cycle 14:10) with food and water *ad libitum*.

Unilateral sciatic nerve lesion and repair were performed on consecutive days, and on each day animals of all experimental groups underwent surgery.

Animals were anesthetized by intraperitoneal injection of chloral hydrate (370 mg/kg body weight; Sigma-Aldrich Chemie GmbH, Steinheim, Germany). To achieve sufficient analgesia, buprenorphine (0.045 mg/kg body weight, Temgesic; Essex Pharma GmbH, Munic, Germany) was intramuscularly applied. Body temperature was monitored and animals were kept on an electric heating pad during anesthesia. The left hind legs were shaved, the skin disinfected, and aseptic techniques used to ensure sterility. The left sciatic nerve was exposed by a skin incision along the femur followed by blunt separation of the biceps femoris and superficial gluteal muscles. The nerve was freed from surrounding connective tissue.

The 2 different sciatic nerve injury and repair models used in this study are depicted in Fig. 1. For nerve crush (crush, n=10) the sciatic nerve was crushed 3 times, for 5 seconds each, using No. 5 Dumont forceps (Fine Science Tools GmbH, Heidelberg, Germany). Afterward, an epineurial window was opened at the lesion site using microscissors (Vannas-Tübingen; Fine Science Tools GmbH, Heidelberg, Germany). Through the incision, the cone tip of a fixed needle plunger protection syringe (26-gauge, SGE GmbH, Griesheim, Germany) was inserted and a 2×20 μL of $C3^{156-181}$ peptide solution or solutions of nerve growth factor (NGF) (reference group 1; Sigma-Aldrich, Taufkirchen, Germany) or $C3^{bot}$-wild-type protein (reference group 2) or of vehicle alone (vehicle control, PBS) injected directly into the crush lesion. The epineurial window was closed with a single epineurial suture (9–0 Ethilon II; Ethicon,

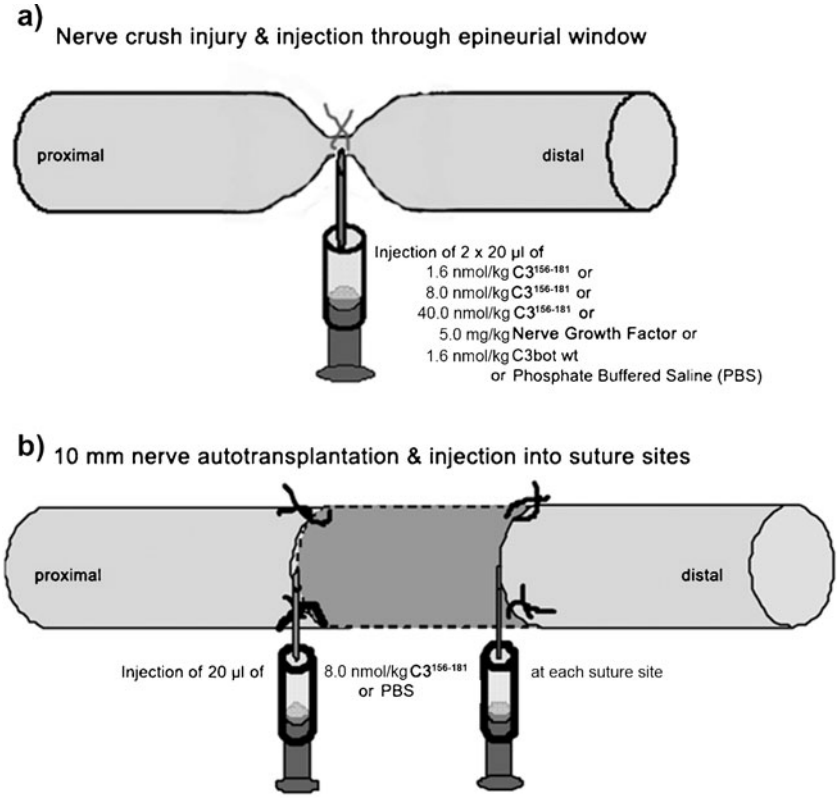

Fig. 1. Schematic drawing of the sciatic nerve injury and repair models used in the presented study. (**a**) After sciatic nerve crush, 1 of 6 different solutions was injected into the crush lesion through an epineurial window, which was closed afterward by a single epineurial suture. (**b**) After bridging a 10-mm sciatic nerve gap with an autotransplant, either vehicle alone or 8 nmol/kg $C3^{156-181}$ was injected into each suture site. PBS=phosphate buffered saline

Norderstedt, Germany). The final treatment dosage was as follows: $C3^{156-181}$ peptide: 1.6 nmol/kg body weight, 8 nmol/kg body weight, or 40 nmol/kg body weight; NGF: 5 mg/kg body weight; $C3^{bot}$-wild-type protein: 8 nmol/kg body weight.

For nerve reconstruction using nerve autotransplantation, the sciatic nerve was transected proximal to its trifurcation into the tibial nerve, the common fibular, and the sural nerve. After reconnection with epineurial sutures (9–0 Ethilon II; Ethicon), the nerve was transected and sutured 10-mm distal to the first transection site again. Into each suture site, 20 µL of 8 nmol/kg body weight $C3^{156-181}$ peptide or vehicle (PBS) were injected, and the sutures covered each with a small strip of absorbable gelatin sponge (Equispon; Equimedical BV, Zwanenburg, The Netherlands) to avoid leakage.

Finally, muscle layers (4–0 Ethilon II) and the skin were sutured (3–0 Dexon; Braun-Dexon GmbH, Spangenberg, Germany). The animals were frequently checked for automutilation and anti-bite spray (Alvetra GmbH, Neumünster, Germany) was applied to the paws or a rat collar (Kent Scientific Corporation, Torrington, CT) used for 1 to 2 days, if necessary. In the following 3 to 10 weeks, Static Sciatic Index (SSI) measurements, as well as the pinch test, were conducted weekly.

Visualization of Drug Distribution by Vital Dye Staining

To asses the distribution of drug delivery in the sciatic nerve crush model, we injected 40 µL of toluidine blue vital dye (1% toluidine blue in 1% $Na_2B_4O_7$ in distilled H_2O) into 5 additional animals. As shown in Fig. 2a and c, the vital dye was distributed along the mean distances of 10 mm into proximal and 6 mm into distal direction from the crush injury and injection sites. The dye was still visible 24 h after injection (Fig. 2b and d). The nerve tissue was then removed, fixed by immersion in 4% paraformaldehyde in 0.1 M phosphate buffer (pH 7.4) overnight in the dark, and freeze protected by immersion in 30% sucrose for 24 h in the dark (+4°C). The tissue was then frozen in Tissue-Tek (O.C.T. Compound; Sakura Finetek, Staufen, Germany) and cut into longitudinal 10-µm thick serial cryostat sections. The sections were mounted on uncoated glass slides and demonstrated that the dye was not only distributed subepineurially, but also in the center of the nerves (Fig. 2e and f).

Evaluation of Motor Recovery

SSI

Functional motor recovery was evaluated for a period of 3 weeks after sciatic nerve crush injury and for as much as 10 weeks after nerve autotransplantation. Only animals with no signs of automutilation were evaluated, and those with slightly reddened toe tips after nail biting were excluded from behavioral tests for 1 or 2 tests. Eventually changes occured in numbers of evaluated animals per group ("see Results for details"). The observers were blinded to

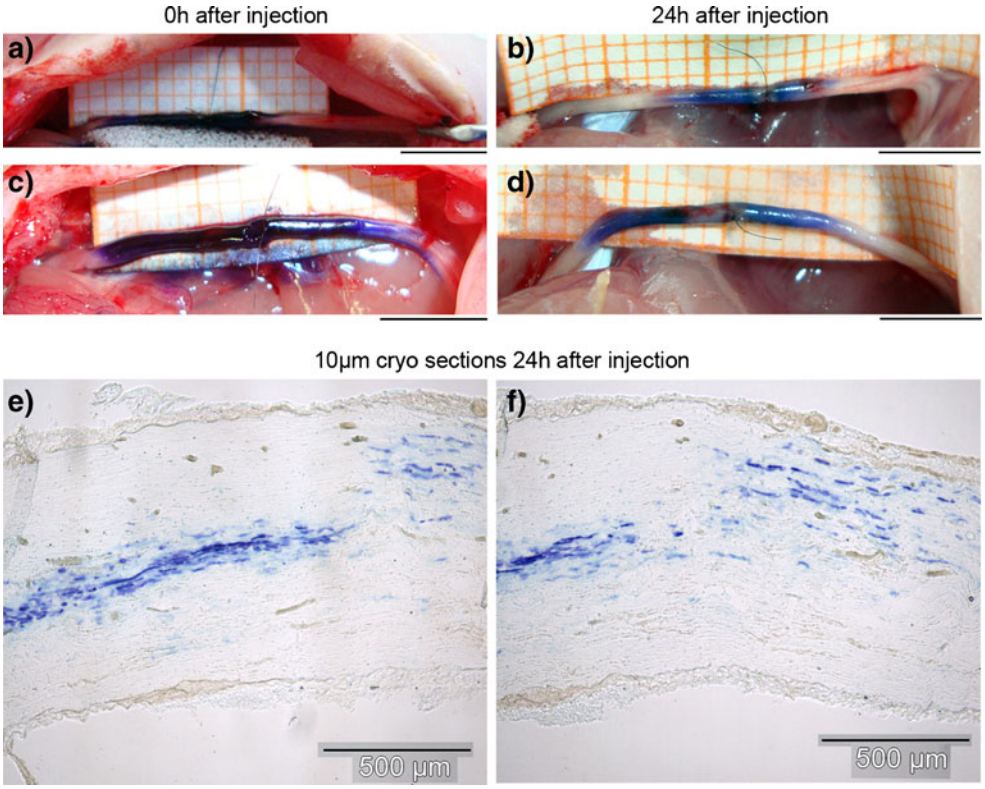

Fig. 2. Results after injection of toluidine vital dye into the crush lesion. Photographs were taken directly (**a**) and (**c**) and 24 h (**b**) and (**d**) after injection of 40 µL of toluidine blue in 2 different nerves. The thin suture marks the closed epineurial window. (**a-d**) Scale bar=5 mm. (**e**, **f**) 10-µm longitudinal cryosections through a third sample revealed that the vital dye was distributed also inside the nerve approximately 10-mm proximal to the injection site

the treatment conditions. After surgery, all animals were numbered consecutively by the operator (K.H.T.) and the animal code was only opened after all measurements were performed and analyzed for each animal.

To evaluate sciatic nerve recovery, toe spread analysis was carried out weekly after surgery. The animals were placed into a Plexiglas box (20 cm x 12 cm x 9 cm, special fabrication Hannover Medical School central research workshops), which restricted their movements within the camera's field of view. The Plexiglas box was fixed on a glass table (Microsoft, Unterschleißheim, Germany). A webcam connected to a notebook was placed under the table. Images of the plantar surface of the animal's paws were then acquired and exported to a freely available image editing program (AxioVision Rel. 4.8; Zeiss, Jena, Germany) for measuring [26]. The parameters of toe spread (distance toe 1–5) and intermediate toe spread (distance toe 2–4) of the operated hind paws(OTS, OITS) and the non-operated hind paws (NTS, NITS) were measured. Then the SSI was calculated by using the following equation (toe spread factor [TSF]; intermediate toe spread factor [ITSF]).

$$\mathrm{TSF} = (\mathrm{OTS} - \mathrm{NTS})/\mathrm{NTS};\ \mathrm{ITSF} = (\mathrm{OITS} - \mathrm{NITS})/\mathrm{NITS}$$
$$\mathrm{SSI} = (108.44 \times \mathrm{TSF}) + (31.85 \times \mathrm{ITSF}) - 5.49.$$

In healthy animals, the SSI is approximately 0 and decreases to −100 after complete impairment of the sciatic nerve.

Electrodiagnostic Measurements

At the end of the observation time, functional reinnervation of the gastrocnemius muscle was analyzed prior to tissue explantation. Therefore, ipsilateral and contralateral sciatic nerves were exposed and electrically shielded on both sides against the surrounding tissue using latex patches. A bipolar hook steel electrode was contacted with the nerve proximal and distal to the suture sites, respectively. Single rectangular stimuli of 0.1-ms duration were pulsed by a software-controlled stimulus generator (2-channel Keypoint Portable EMG-System, Keypoint GmbH, Düsseldorf, Germany). The stimulus intensity was gradually raised from the threshold of a minimum response to a level of 30% greater than the maximum response (not greater than 8 mA). To determine threshold current intensities, current intensity was raised from 0 mA in gradual steps of 0.1 mA (0–2 mA) or 0.2 mA (2 mA and greater), and in parallel elicited compound muscle action potentials (CMAPs) were recorded from the gastrocnemius muscle (bipolar electromyography needle electrodes inserted into the tendon and the belly) and were depicted on the screen of a notebook connected to the Keypoint Portable EMG-System (Keypoint GmbH). CMAPs or evoked hind-paw movements were ranked as signs for successful reinnervation.

The term "evoked hind-paw movements" describes the spreading of the lateral toes of a hind-paw on direct electrodiagnostical nerve stimulation [21, 25]. The movement also includes the gastrocnemius muscle, which

potentially initiated backward movement of the hind paw, together with toe spreading movements. The different strength of the evocable movements was ranked using a 3-step score system (score 1=twitching of gastrocnemius muscle with no visible movement of the paw or toes; score 2=twitching of gastrocnemius muscle plus slight movement of the paw or toes; and score 3=strong movements).

Furthermore, whenever CMAPs could be recorded, threshold current intensities, as well as maximal CMAP amplitudes, their latencies and current were determined, and the motor nerve conduction velocity was calculated. Electrodiagnostical measurements of the contralateral non-operated sciatic nerve served as an internal reference.

Gastrocnemius Muscle Weight Ratio

After electrodiagnostical evaluation the gastrocnemius muscle, together with the adjacent soleus muscle, was dissected, and the weight was determined for both the leg ipsilateral and the leg contralateral to the injury. The gastrocnemius muscle weight ratio (*g*)ipsilateral divided by (*g*)contralateral indicates the value of recovered muscle mass due to reinnervation by motor axons.

Nerve Morphometry

On explantation, the regenerated nerve tissue was transected at 4-mm distal to the crush lesion or 1-mm distal to the distal nerve suture, respectively. The sutures closing the epineurial window at the crush lesion site or those connecting the distal nerve stumps to the autotransplant were still visible as landmarks. The regenerated nerve tissue was transferred in a fixative according to Karnovsky (2% paraformaldehyde, 2.5%glutaraldehyde in 0.2 M sodium cacodylate buffer, pH 7.3 [18, 20] for 24 h, then rinsed 3 times with 0.1 M sodium cacodylate buffer containing 7.5% sucrose prior to postfixation in 1% OsO_4 for 1.5 h). Myelin staining was performed as previously described [18, 20], 24 h in 1%potassium dichromate, followed by 24 h in 25% ethanol, and for another 24 h in hematoxylin (0.5 in 70% ethanol). After dehydration, the tissue was epon-embedded and semi-thin (1-μm) cross sections were cut with glass knives (Ultramikrotome System, 2128 Ultrotome; LKB, Bromma, Sweden) mounted on uncoated glass slides and stained with toluidine blue to further enhance the myelin staining [18, 20].

Regenerated myelinated axons (mAx) were analyzed at defined points of the regenerated nerve tissue ("see Results for details"). The semi-thin cross sections were digitalized using an Olympus BX60 microscope (Olympus, Hamburg, Germany) at 40x magnification at 1288 x 966 DPI, aligning single pictures to total cross sections using Cell^P (multiple image alignment, Olympus, Hamburg, Germany), and finally analyzed using AnalySISPro 3.1/3.2 (Soft Imaging System GmbH, Hamburg, Germany) [20, 27].

Because of the large size of the cross sections, the number of mAx was determined only in defined parts of the entire cross sections [25, 28], followed by measuring the cross-sectional area and extrapolation to the total number of mAx. The number of mAx was set in relation to the whole cross-sectional area to calculate the nerve fiber density (mAx/mm²). The *g*-ratio, an index for the grade of axon myelination, which is determined by the axon diameter divided by the total fiber diameter, was evaluated for at least 200 mAx of each section [20, 27] by an indirect calculation using the following formula: *g*-ratio=axonal diameter of myelinated fibers/(axonal diameter of myelinated fibers+2x myelin thickness).

All quantification was done by an observer blinded to the experimental conditions. Blinding was achieved by consecutive numbering of each nerve sample. Numbers were different to animal numbers used before and given by persons different from the operator and observers. The number code was only opened after histomorphometrical analysis was completed for all samples.

Detection of Active RhoA within the Sciatic Nerves by Immunoprecipitation

To assess a RhoA inactivation induced by $C3^{156\text{-}181}$ peptide solution or $C3^{bot}$-wild-type protein within the lesioned and treated rat sciatic nerve, we performed crush lesion and injection of 40 μL solution in 12 additional animals. The injected solutions were as follows: PBS (n=4), 8 nmol/kg body weight $C3^{156\text{-}181}$ peptide (n=4) or 8 nmol/kg body weight $C3^{bot}$-wild-type protein (n=4). The highest level of activated RhoA in the sciatic nerve has been detected before at 3 days after surgery [29], therefore we chose the same timeframe for this additional experiment. Three days after surgery, the animals were sacrificed and 2 cm of the sciatic nerves rapidly dissected, dried-frozen in liquid nitrogen, and stored at −80°C. The 2-cm samples were cut out proximal to the crush lesion (marked by a suture) from the left nerves, and accordingly from the contralateral noninjured nerves as well.

For immunoprecipitation, samples were pooled from 4 animals/condition and sonicated in 1 mL immunoprecipitation buffer (20 mM Tris HCl pH 7.2, 50 mM NaCl, 3 mM MgCl, 1%NP40, 100 μM phenylmethylsulfonylfluorid (PMSF), 1%protease inhibitors) on ice. Solubilized tissue was spun down at 13,000*g* for 10 minutes at 4°C. Immunoprecipitation of GTP-RhoA (guanosin-5'-triphosphat bound RhoA) was done for 45 minutes in 4°C using 1 μL antibody (NewEast Biosiences, Malvern, PA, USA), followed by incubation with 50 μL protein A/G PLUS-agarose beads (Santa Cruz Biotechnology, Heidelberg, Germany) for 45 minutes. Agarose beads were spun down

at 10,000*g* for 5 minutes, washed 2 times with immunoprecipitation buffer and re-suspended in SDS-PAGE sample buffer. Beads Proteins were separated by SDS-PAGE (sodium dodecyl sulfate polyarylamide gel electrophoresis) (15% acrylamide) followed by Western blot analysis with mouse anti-RhoA (1:200; Santa Cruz Biotechnology). Finally, all signals were analyzed densitometrically using the Kodak 1D Image Analysis Software (Eastman Kodak Company, Stuttgart, Germany) and normalized to β-actin signals.

Statistical Analysis

For statistical analysis, GraphPad InStat Software, version 3.06 for Windows (GraphPad Software Inc., San Diego, CA) was used. Data from different groups were compared pair-wise. This was done with the unpaired *t*-test for data that passed the normality test, and the nonparametric Mann-Whitney *U* test was chosen for data that did not pass the normality test ("see Results for details").

For the autotransplant experiments, the 1-tailed *p* value was calculated for analyzing the straightforward hypothesis that $C3^{156-181}$ would support axonal and functional nerve regeneration in comparison to PBS. The χ^2 distribution (percentage of animals/group) of values above the median of the control group (PBS) was analyzed where single values indicated a difference between the control group and the group that was treated with $C3^{156-181}$. The *p* values with $p<0.05$ were taken as statistically significant. The respective statistical test used is indicated in the result section.

Results

Treatment with $C3^{156-181}$ Speeds up Motor Recovery after Nerve Crush Injury

To assess the motor nerve regeneration after crush injury, the SSI was calculated weekly. First significant differences in the SSI were detected 2 weeks after surgery (Mann-Whitney *U* test; $p<0.05$) between the vehicle alone group (PBS) and the high dosage $C3^{156-181}$ group (40 nmol/kg), see Fig. 3a. At 3 weeks after surgery, SSI values did significantly increase in comparison to the 2 weeks values in the NGF reference group as well as all $C3^{156-181}$ groups (1.6 nmol/kg, 8 nmol/kg, 40 nmol/kg). Furthermore, in comparison to the PBS group value, the SSI values of the 8 nmol/kg $C3^{156-181}$ group and the 40 nmol/kg $C3^{156-181}$ group were significantly increased (Mann-Whitney *U* test). All results of the SSI calculation from 1 week before surgery to 3 weeks after surgery and the gastrocnemius muscle weight ratios are listed in Table 1.

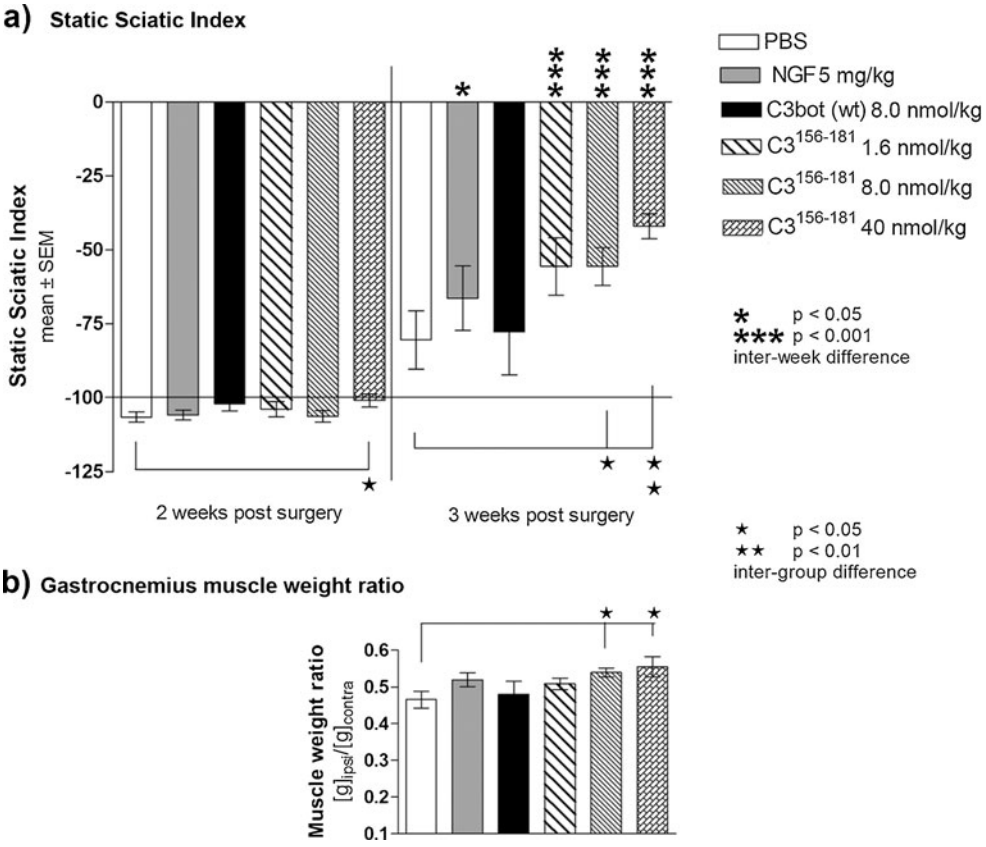

Fig. 3. Analysis of motor recovery after nerve crush injury, as evaluated by the Static Sciatic Index (SSI) and calculation of the gastrocnemius muscle weight ratio. (**a**) Mean± SEM values of the SSI determined 2 weeks and 3 weeks after surgery. A significant difference to the phosphate buffered saline (PBS) control group is seen at first in the 40 nmol/kg $C3^{156-181}$ group 2 weeks after surgery. Best motor recovery is indicated in the $C3^{156-181}$-treated groups at 3 weeks after surgery. (**b**) The mean±SEM value of the gastrocnemius muscle weight ratio is correlated to the motor recovery level determined by the SSI. Treatment with 8.0 nmol/kg and 40 nmol/kg $C3^{156-181}$ significantly improved the obtained regeneration values. NGF=nerve growth factor

Table 1. Study I – Crush Injury*

Study I – crush	Experimental group					
	PBS Reference 1	NGF Reference 2	$C3^{bot}$ (wt) 8.0 nmol/kg	$C3^{156-181}$ 1.6 nmol/kg	$C3^{156-181}$ 8.0 nmol/kg	$C3^{156-181}$ 40 nmol/kg
Static sciatic index pre- surgery	−1.84±2.36	−3.42±2.13	−2.75±7.95	−11.02±4.07	−7.18±3.58	−10.35±3.90
	n=8	n=7	n=8	n=7	n=8	n=8
1-week postsurgery	−103.20±1.80	−103.82±3.12	−100.07±2.83	−98.87±3.10	−105.50±1.64	−98.58±2.10
	n=8	n=7	n=8	n=7	n=8	n=8
2-weeks postsurgery	−106.68±1.71	−106.02±1.65	−102.19±2.40	−104.03±2.59	−106.43±1.95	−101.06±2.22†
	n=8	n=7	n=8	n=7	n=8	n=8
3-weeks postsurgery	−80.55±9.87	−66.46±10.94	−77.82±14.60	−55.69±9.75	−55.66±6.38†	−42.05±4.27‡
	n=7	n=7§	n=8	n=7¶	n=8¶	n=8¶
Gastrocnemius muscle weight ratio	0.47±0.02	0.52±0.02	0.48±0.035	0.51±0.02	0.54±0.01†	0.55±0.03†
3-weeks postsurgery	n=8	n=7	n=8	n=7	n=8	n=8

n number of animals tested; *NGF* nerve growth factor; *PBS* phosphate buffered saline

*Results from analyses of motor behavior, as determined by the Static Sciatic Index and by calculating the gastrocnemius muscle weight ratio. Data are presented as mean±SEM. Statistical analysis was done by using the Mann-Whitney *U* test

† $p<0.05$

‡ $p<0.01$ indicating significant differences between the phosphate buffered saline group values and the $C3^{156-181}$ group values evaluated at the same time after injury

§ $p<0.05$

¶ $p<0.001$ indicating significant inter-week differences (2-weeks values *vs* 3-weeks values) within one group of animals

Figure 3b illustrates that the motor recovery level, indicated by the SSI, did correlate to the gastrocnemius muscle weight ratio ([g]ipsilateral/[g]contralateral) determined 3 weeks after surgery. The muscle weight ratios of the 8.0 nmol/kg $C3^{156-181}$ group and the 40 nmol/kg $C3^{156-181}$ group were significantly higher than in the PBS group.

Three weeks after surgery electrodiagnostical evaluation was performed in all groups. The results of the electrodiagnostical evaluation are summarized in Table 2. The ipsilateral mean threshold current intensities, the ipsilateral mean latencies of the maximal evocable CMAPs, as well as the mean maximal CMAP amplitudes differed significantly to the values obtained from the contralateral healthy control nerves ($p<0.001$-0.05, Mann-Whitney *U* test). Although no statistically significant differences were detectable between the experimental groups, it is noteworthy that the

Table 2. Study I – Crush Injury*

		Current intensity (mA)		Maximal CMAP	
		Threshold	Maximal	Latency (ms)	Amplitude (mV)
Contralateral	All (n=36)	0.11±0.01†	0.76±0.14	1.64±0.06‡	55.74±1.98‡
Ipsilateral	PBS (n=4)	0.38±0.11	0.95±0.69	5.3±0.31	4.73±1.29
	NGF (n=6)	0.22±0.04	1.0±0.45	4.88±0.84	4.40±0.77
	C3bot (wt) (n=4)	0.3±0.11	1.38±0.55	4.63±0.48	5.58±0.80
	$C3^{156-181}$ 1.6 nmol/kg (n=6)	0.27±0.07	1.62±0.37	5.3±0.46	4.27±0.68
	$C3^{156-181}$ 8.0 nmol/kg (n=8)	0.26±0.06	0.84±0.26	5.51±0.22	5.64±0.35
	$C3^{156-181}$ 40 nmol/kg (n=8)	0.21±0.04	0.73±0.28	4.88±0.28	4.90±0.72

CMAP compound muscle action potential; *n* number of animals tested

*Current intensity, latency and amplitude (mean±SEM) for the threshold and maximal CMAP at the day of explantation, 3 weeks after crush injury. Statistical analysis was done by using the Mann-Whitney *U* test

† $p<0.05$

‡ $p<0.001$ indicating significant differences between contralateral control values and ipsilateral values of all groups investigated

40 nmol/kg $C3^{156-181}$group had the lowest mean threshold current intensity as well as the lowest mean current intensity needed to elicit the maximal CMAP amplitude.

Treatment with $C3^{156-181}$ after Nerve Crush Injury Increases Regeneration of Myelinated Axons in a Dose-Independent Way

Semi-thin nerve cross sections, harvested 4 mm distal to the crush lesion 3 weeks after surgery, were morphometrically analyzed. As depicted in Fig. 4a, the nerve fiber density differed significantly (unpaired t-test, Welch corrected) between several groups. In the $C3^{156-181}$ treated groups axonal regeneration was significantly increased in comparison to the PBS group. Furthermore, in the 1.6 nmol/kg $C3^{156-181}$ group and the 8.0 nmol/kg $C3^{156-181}$ group, significantly more myelinated axons per mm^2 regenerated than in the NGF and the $C3^{bot}$ (wt) reference groups. It is noteworthy that the highest nerve fiber density was detected in the group treated with only 1.6 nmol/kg $C3^{156-181}$. Representative photomicrographs of nerve cross sections are presented in Fig. 4 for PBS (Fig. 4b) and 1.6 nmol/kg $C3^{156-181}$ (Fig. 4c) treated animals. Although in all sections signs of axonal degeneration (onion bulb formations) were still visible 4 mm distal to the crush at 3 weeks after surgery, the different degree of regeneration of myelinated axons was evident. More results from the morphometrical analysis of semi-thin nerve cross sections harvested 4-mm distal to the crush lesion 3 weeks after surgery are summarized in Table 3.

Beside the nerve fiber density no other analyzed parameter differed significantly between the groups. A tendency however, to increased axonal diameters in the $C3^{156-181}$ treated groups appeared in comparison to the other conditions (highest value in the 40 nmol/kg-$C3^{156-181}$group).

Treatment with 8.0 nmol/kg $C3^{156-181}$ after 10-mm Nerve Autotransplantation Speeds Up Reinnervation of Hind-Limb Muscles and Increases Motor Function

While after 10-mm nerve autotransplantation the evaluation of the SSI demonstrated almost no recovery and no differences between the analyzed conditions, significant differences could be detected with other test paradigms.

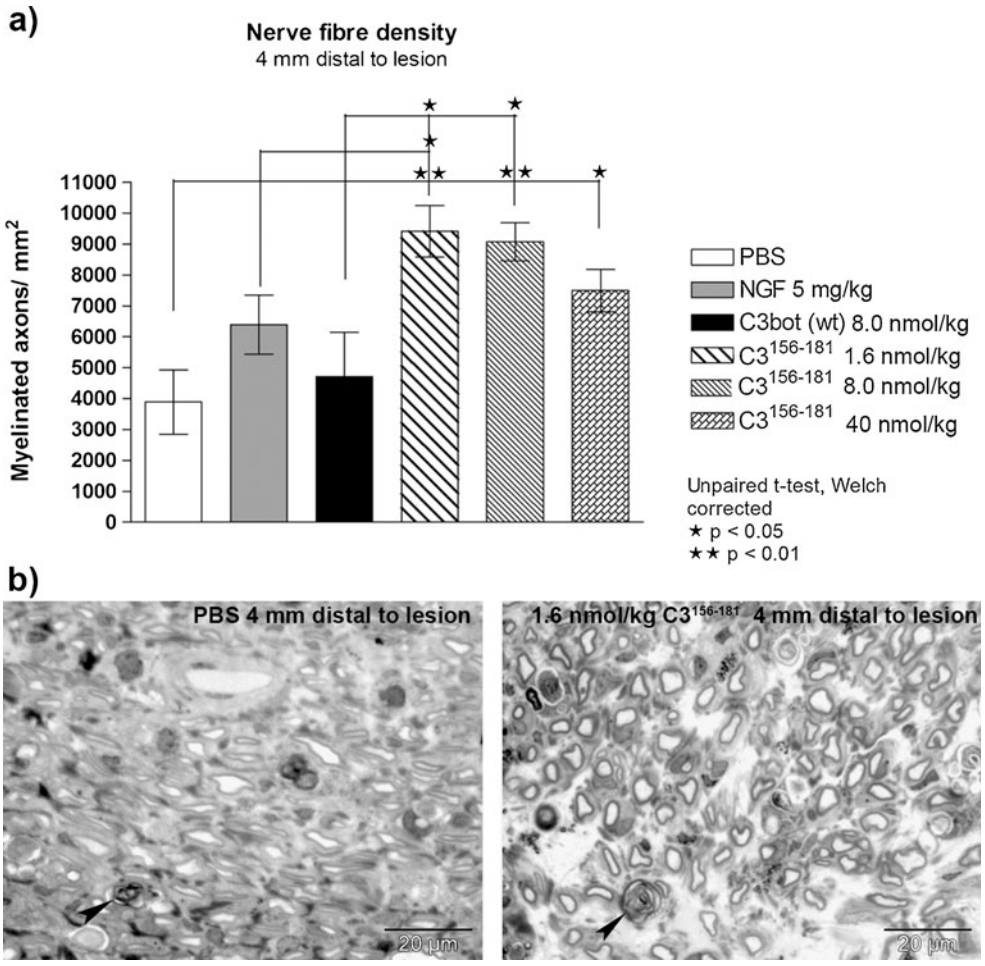

Fig. 4. Nerve fiber densities as determined by nerve morphometry 4-mm distal to the crush lesion at 3 weeks after surgery. (**a**) Bar graph depicting the number of regenerated myelinated axons/mm^2. Treatment with $C3^{156-181}$ significantly increased axonal regeneration. (**b**) and (**c**) Details of semi-thin cross section through regenerated nerves after phosphate buffered saline (PBS) (**b**), or 1.6 nmol/kg $C3^{156-181}$ (**c**) treatment. Arrowheads point to onion bulb formations of degenerated axons that are still present. Scale bar=20 µm. NGF=nerve growth factor

Table 3. Study I – Crush Injury*

Study I – crush	Experimental group					
	PBS Reference 1	NGF Reference 2	$C3^{bot}$ (wt) 8.0 nmol/kg	$C3^{156-181}$ 1.6 nmol/kg	$C3^{156-181}$ 8.0 nmol/kg	$C3^{156-181}$ 40 nmol/kg
Myelinated axons/mm^2	3887±1036 n=7	6393±956 n=5	4714±1434 n=8	9412±836 n=7 †*vs* NGF+$C3^{bot}$ ‡*vs* PBS	9071±617 n=8 †*vs* NGF ‡*vs* PBS	7492±689 n=6 †*vs* PBS
Axonal area	3.17±0.13 μm^2 n=6	3.61±0.42 μm^2 n=4	3.43±0.33 μm^2 n=7	3.70±0.39 μm^2 n=7	3.44±0.21 μm^2 n=7	3.66±0.42 μm^2 n=5
Axonal diameter	2.87±0.11 μm	2.98±0.12 μm	2.72±0.15 μm	3.10±0.12 μm	3.11±0.05 μm	3.13±0.08 μm
Myelin thickness	0.88±0.07 μm n=3	0.77±0.11 μm n=4	0.85±0.07 μm n=6	0.91±0.05 μm n=5	0.90±0.05 μm n=4	0.85±0.09 μm n=4
g Ratio	0.51±0.03	0.59±0.04	0.50±0.02	0.51±0.01	0.50±0.01	0.55±0.03

n number of animals tested; *NGF* nerve growth factor; *PBS* phosphate buffered saline

*Results of the morphometrical analysis of regenerated myelinated axons 4-mm distal of the crush lesion at 3-weeks postsurgery. Data are presented as mean±SEM. Statistical analysis was done with the unpaired *t* test after Welch correction

† $p<0.05$

‡ $p<0.01$ indicating significant differences between the groups as listed

During the Early Phase of Regeneration (4 weeks) $C3^{156-181}$ Promotes Axonal Elongation into Motor Targets and Reduces Axonal Sprouting

During the 4-week observation period the size of the regenerating gastrocnemius muscle did not increase to values allowing recording of CMAPs. However, electrical stimulation of the regenerated nerve proximal to the autotransplant did result in visible movements evoked by the stimulation such as twitching of the gastrocnemius muscle (score 1) or as a progression backward movement of the paw or toe spreading movements (score 2). Very strong movements or combined movements were given a score 3 value. A score of 0 indicated no evocable movement. As depicted in Fig. 5a treatment with $C3^{156-181}$ resulted in evocable movements with higher scores than treatment with PBS vehicle alone. Figure 5b illustrates the results of calculating the gastrocnemius muscle weight ratio ([g]ipsilateral/[g]contralateral) 4 weeks after surgery. Significantly more animals of the $C3^{156-181}$ group displayed muscle weight ratios above the median of the PBS control group (0.325, χ^2 distribution of animals per group [%]).

As depicted in Fig. 5c, calculation of the nerve fiber density at 1-mm distal to the autotransplant revealed, during the first 4 weeks after surgery, that significantly less myelinated axons per mm^2 regenerated in the $C3^{156-181}$ group than in the PBS group (χ^2 distribution of animals per group [%] with values greater than the median of the PBS control group). No other morphometrical differences could be detected 4 weeks after surgery. Complete results from the morphometrical analysis of semi-thin nerve cross sections harvested 4 or 10 weeks after surgery are summarized in Table 4.

Treatment with 8.0 nmol/kg $C3^{156-181}$ Increases Nerve Functionality 10 Weeks after 10-mm Nerve Autotransplantation

During a period of 10 weeks after autotransplantation, the gastrocnemius muscle mass did increase to a size allowing electrodiagnostical evaluation of the regeneration status. The results of the electrodiagnostical evaluation are summarized in Table 5.

Ten weeks after surgery both groups differed significantly in their ipsilateral maximal current intensity, the latency of the maximal evocable compound muscle action potential (CMAP), as well as the maximal CMAP amplitude to the values obtained from the contralateral healthy control nerves (Mann-Whitney *U* test, 2-tailed *p* value). There were no intergroup differences detectable, except the following. Calculation of the 1-tailed *p* value following the hypothesis that $C3^{156-181}$ treatment promotes motor recovery detected a significantly ($p<0.05$) higher mean maximal CMAP amplitude in the $C3^{156-181}$ group (22.68±2.76 mA) in comparison to the PBS control group (16.68±1.61 mA). Analyzing the χ^2-distribution of animals per group (percentage), which

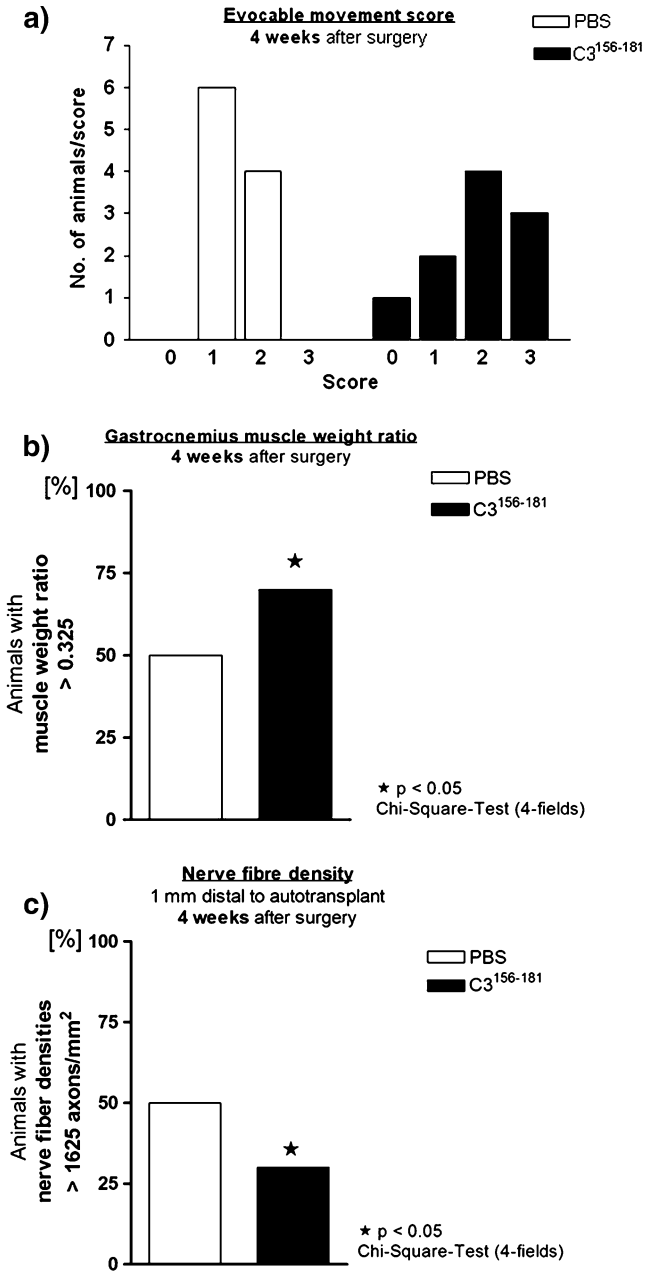

Fig. 5. Analysis of regeneration parameters 4 weeks after 10-mm nerve autotransplantation. (**a**) Bar graph depicting a significant right shift of the evocable movement score after treatment with $C3^{156-181}$. (**b**) Four weeks after surgery, significantly more animals of the $C3^{156-181}$ group, as in the phosphate buffered saline (PBS) group displayed a gastrocnemius muscle weight ratio greater than the control group median. (**c**) The density of regenerated myelinated axons at 1-mm distal to the autotransplants at 4 weeks after surgery was significantly reduced after $C3^{156-181}$ treatment

displayed a motor nerve conduction velocity ratio greater than the median value of the PBS control group (0.51), further indicated significantly better motor nerve function in the $C3^{156-181}$ group (Fig. 6a). The gastrocnemius muscle weight ratio was 10 weeks after autotransplantation no longer different between the PBS control group (0.50±0.07) and the $C3^{156-181}$ group (0.49±0.08).

Increased Nerve Functionality after Treatment with $C3^{156-181}$ is Related to Increased Axonal Diameters and Myelin Thickness

Again, the regenerated nerve tissue was morphometrically analyzed 1-mm distal to the autotransplant (see Table 5). The groups were statistically compared with regard to the χ^2 distribution of animals per group (percentage), with values greater than the median of the PBS control group.

Ten weeks after autotransplantation, the number of regenerated myelinated axons per mm^2 was no longer different between the groups. Additionally, the axonal area was similar in both groups. However, axonal diameter (Fig. 6b) and myelin thickness (Fig. 6c) showed significant differences in the χ^2 distribution, indicating increased axonal maturation 10 weeks after treatment with 8 nmol/kg $C3^{156-181}$. The *g*-ratio was similar in both groups, demonstrating that the regenerated myelinated axons displayed a myelin thickness appropriate to their diameter.

$C3^{156-181}$ Peptide Modulates Active RhoA Levels *in Vivo*

To elucidate the activity of the $C3^{156-181}$ peptide *in vivo*, active RhoA levels have been measured in an immunoprecipitation experiment in the proximal sciatic nerve. It has been demonstrated before that a lesion of rat sciatic nerves results in RhoA activation proximal to the lesion sites [29]. Figure 7 illustrates that treatment with $C3^{156-181}$ and $C3^{bot}$ wt peptide prevented this activation in comparison to the treatment with PBS alone. The lower level in Fig. 7a gives the input of β-actin and the middle level the input of RhoA into the Western blot experiment; the upper level gives the active GTP-RhoA. Figure 7b depicts the ratio between total RhoA input and activated GTP-RhoA levels (both normalized against β-actin). Three days after crush lesion and treatment with PBS, $C3^{156-181}$ peptide (8 nmol/kg), or $C3^{bot}$-wild-type protein (8 nmol/kg), the levels of active GTP-RhoA were clearly reduced in ipsilateral and contralateral sciatic nerve samples from the $C3^{156-181}$ peptide and $C3^{bot}$-wild-type protein-treated groups in comparison to the PBS-treated group.

Discussion

This study provides the first evidence that a single administration of the short $C3^{bot}$-derived 26 amino-acid fragment $C3^{156-181}$ is sufficient to promote peripheral nerve regeneration after injury of different severity by enhancing axonal elongation into appropriate targets followed by

Table 4. Study II – Nerve Autotransplant*

Study II Nerve autotransplant	Experimental group			
	PBS - 4 weeks Reference	$C3^{156-181}$ - 4 weeks 8.0 nmol/kg	PBS - 10 weeks Reference	$C3^{156-181}$ - 10 weeks 8.0 nmol/kg
Myelinated axons/ mm^2	n=10	n=10	n=10	n=10
	1533±196	1420±320	14,021±1108	14,797±983
Axonal area	2.95±0.30 μm^2	3.88±0.60 μm^2	4.62±0.18 μm^2	4.76±0.20 μm^2
Axonal diameter	2.24±0.10 μm	2.45±0.16 μm	2.74±0.07 μm	2.73±0.14 μm
Myelin thickness	n=5	n=5	n=10	n=7
	0.65±0.02 μm	0.63±0.04 μm	0.72±0.04 μm	0.78±0.04 μm
g ratio	n=5	n=5	n=10	n=10
	0.66±0.004	0.68±0.02	0.64±0.02	0.64±0.02

n number of animals tested; *PBS* phosphate buffered saline

*Results of the morphometrical analysis of regenerated myelinated axons 1-mm distal to an autotransplant at 4 weeks and 10 weeks postsurgery. Data are presented as mean±SEM

increased axonal maturation, which results in fast and substantial functional motor recovery.

Support of Axonal Elongation and Maturation Instead of Sprouting by $C3^{156-181}$

The axonotrophically active region of the clostridial $C3^{bot}$ wild-type protein has been identified to be localized within the amino acids 154–182 of $C3^{bot}$ [30]. The 29 amino-acid fragment $C3^{154-182}$ promoted axonal outgrowth from organotypic hippocampal slice cultures into entorhinal slice cultures [30] *in vitro*. Furthermore, $C3^{154-182}$ has recently been shown to increase axonal outgrowth across spinal cord injuries and to improve functional recovery after such injuries [24]. The enzymatic RhoA inactivation by the ADP (adenosindiphosphat)-ribosyltransferase activity of $C3^{bot}$ wild-type protein is long known [31], but it has also been shown before that enzyme-deficient $C3^{bot}$ mutants ($C3^{bot}$E174A, $C3^{bot}$E174Q) are equally efficient in stimulating axonal outgrowth from hippocampal neuron cultures [32]. Although the $C3^{154-182}$ region does not posses enzymatic activity, a RhoA inactivating function mediated via an (as yet) unknown mechanism could not be fully excluded until now, and RhoA is known to be crucially involved in actin and microtubule dynamics [24]. Pull-down experiments have shown a reduction of active RhoA levels in primary cultures of embryonic hippocampal neurons *in vitro* after incubation with $C3^{154-182}$ for 4 days. We used the further shortened 26 amino acid fragment $C3^{156-181}$ in the current study, which showed the same effects as the longer 29 amino acid peptide *in vitro*.

We attribute the effect of $C3^{156-181}$ on axonal elongation and maturation presented here to the residual RhoA inactivation. After injury, an up-regulation of activated RhoA is detected in the axons within the proximal nerve [29]. It has further been postulated that this RhoA activation accounts as a pause signal for axonal outgrowth [33]. As such the RhoA inactivation is eventually the basis for the so-called staggered outgrowth of regenerating axons for a period of as much as 10 weeks after injury, in which regenerating neurons

Table 5. Study II – Nerve Autotransplant

		Current intensity (mA)		Maximal CMAP	
		Threshold	Maximal	Latency (ms)	Amplitude (mV)
Contralateral	All (n=19)	0.35±0.24	0.67±0.22†	2.33±0.23†	52.22±4.69†
Ipsilateral	PBS 10 weeks (n=10)	0.63±0.5	1.87±0.32	3.42±0.28	16.68±1.61
	$C3^{156-181}$ 8.0 nmol/kg 10 weeks (n=9)	0.78±0.32	1.73±0.4	3.27±0.33	22.68±2.76‡

n number of animals tested; *CMAP* compound muscle action potential

*Current intensity, latency, and amplitude (mean±SEM) for the threshold and maximal CMAP at the day of explantation, 10 weeks after nerve autotransplantation. Statistical analysis was done with the Mann-Whitney *U* test

† $p<0.01$ indicating significant differences between contralateral control values and ipsilateral values of all groups investigated

‡ $p<0.05$ indicating the calculation of a 1-tailed p value revealed statistical differences between PBS- and $C3^{156-181}$ -values

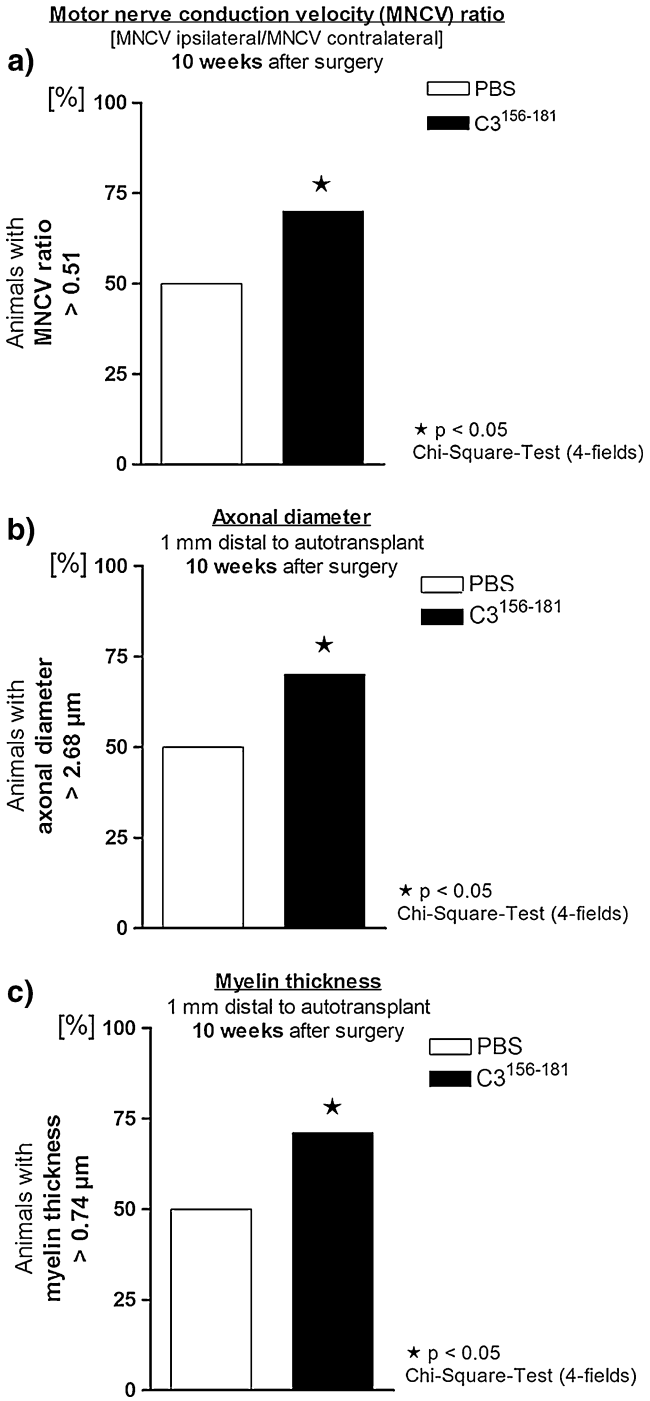

Fig. 6. Analysis of regeneration parameters at 10 weeks after 10-mm nerve autotransplantation. (**a**) 10 weeks after surgery significantly more animals of the $C3^{156-181}$ group, as in the phosphate buffered saline (PBS) group displayed a motor nerve conduction velocity ratio greater than the control group median. (**b**) and (**c**) Nerve morphometry at 1-mm distal to the autotransplants 10 weeks after surgery. Treatment with 8.0 nmol/kg $C3^{156-181}$ significantly increased axonal diameters (**b**) and myelin thickness (**c**) of the regenerated myelinated axons

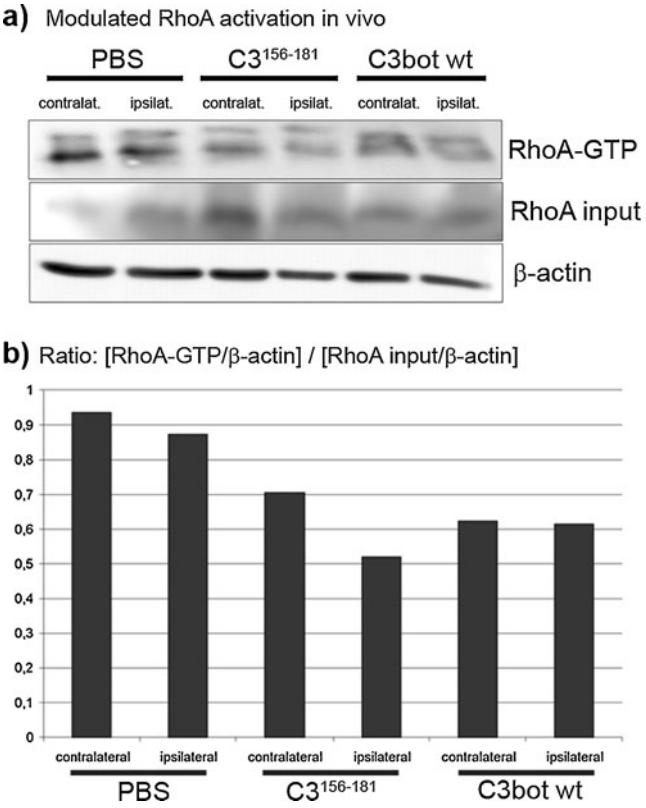

Fig. 7. Prevention of RhoA activation *in vivo* by $C3^{156-181}$ peptide or $C3^{bot}$-wild-type protein. (**a**) GTP-RhoA immunoprecipitation and Western blot analysis demonstrating reduced levels of active GTP-RhoA in contralateral and ipsilateral sciatic nerves after treatment with $C3^{156-181}$ peptide and $C3^{bot}$-wild-type protein in comparison to phosphate buffered saline (PBS) treatment. (**c**) Densitometry and normalization against β-actin allowed the calculation of the ratio between total RhoA input (middle level) in (**b**) and GTP-RhoA levels (upper level) in (**b**). The bar graph underscores the prevented activation of RhoA by treatment with $C3^{156-181}$ peptide or $C3^{bot}$-wild-type protein in contrast to application of PBS

subsequently start to re-grow their axons [33, 34]. Staggered axonal outgrowth reduces the chance for timely and full recovery after severe peripheral nerve injury. Treatment of sciatic nerve crush injuries in mice with the synthetic Rho-kinase inhibitor fasudil (HA-1077) facilitated the maturation of regenerating myelinated axons, as indicated by increased mean fiber diameters and decreased regenerating fiber densities [33]. The same effect is seen in the current study after treatment with $C3^{156-181}$.

Possible Mechanism Underlying the Increased Motor Recovery Induced by $C3^{156-181}$

It has further been shown that RhoA is activated after peripheral nerve injury in motor neurons and dorsal root ganglia, but not in Schwann cells [29, 33]. A significant increase of CMAP amplitudes indicative for better motor recovery was seen in fasudil treated mice after crush injury [33]. Treatment with $C3^{156-181}$ also resulted in improved motor recovery. Our results, together with the shown enzyme-independent inactivation of RhoA by $C3^{154-182}$

[24] makes it likely that a motoneuron specific inactivation of RhoA underlies the regeneration promoting effects of $C3^{156-181}$ in the current study. Active RhoA in neurons functions as the antagonist to the inductors of neurite outgrowth (Rac and Cdc42), and it stops axonal growth and further induces growth cone collapse [31]. The inactivation of RhoA by $C3^{bot}$ catalyzed ADP-ribosylation or by the Rho-kinase inhibitor fasudil, therefore, supports axonal outgrowth after central [35] or peripheral nerve injury [29, 33]. In the current study, treatment with $C3^{156-181}$ increases axonal elongation and reconnection to appropriate targets (functional motor recovery) via a not-yet known pathway. The fact that 1-time administration is sufficient to enhance repair, however, indicates an initial beneficial effect of $C3^{156-181}$-peptide based on the inactivation of RhoA.

Advantage of $C3^{156-181}$ over $C3^{bot}$ Wild Type

Stimulation of axonal outgrowth and maturation accompanied by accelerated motor recovery has also been demonstrated before for the treatment of sciatic nerve crush injuries with NGF by injection of NGF solution into the crush sites [36]. Therefore, treatment with NGF was chosen as a reference condition in the crush injury model used in the current study, but treatment with $C3^{156-181}$ demonstrated a higher potential to increase peripheral nerve regeneration. The mode of NGF action does not involve inactivation of RhoA but a trophic action on the regenerating neurons mediated via the low-affinity nerve growth factor receptor [37]. Currently no receptor for C3 peptides or $C3^{bot}$ is known, and we can only speculate with regard to the RhoA inactivation by C3 peptides (e.g., a direct influence on RhoA by the internalized peptide [24]). The treatment with $C3^{156-181}$ showed a higher potential to increase peripheral nerve regeneration than treatment with $C3^{bot}$-wild-type protein. This indicates that the action of $C3^{156-181}$ is more neuron-specific. Classical pathways of enzymatic RhoA inactivation, as known for the $C3^{bot}$-wild-type protein, do not selectively act on neurons and axons, but also do affect central glial cells [38, 39]. The glial reaction strictly depends on the classical pathway and is not seen with enzyme-deficient $C3^{bot}$ mutants or the C3 peptides [39]. In the current study, axonal and functional regeneration parameters after treatment with $C3^{bot}$-wild-type protein are significantly behind those after treatment with $C3^{156-181}$. This indicates that the treatment with $C3^{bot}$-wild-type protein additionally activates other mechanisms, such as a central glia reaction, which possibly negatively influences neuronal regeneration processes. To date an effect on peripheral glia cells, Schwann cells, has not been demonstrated and has to be the subject of future studies. However, the promoting effect of $C3^{156-181}$ on peripheral nerve regeneration could not only be direct, but also indirectly meditated by Schwann cells. The Schwann cells create a regeneration-promoting milieu [4, 10] and they might be influenced by $C3^{156-181}$ to do so faster and more successful than usual.

Conclusion

Our data indicate that $C3^{156-181}$ is a possible therapeutic agent to support functional recovery after peripheral nerve injury and repair, especially the demonstrated regeneration-promoting effects, that appeared after a single application, make a therapeutic use easy to transfer in a clinical setting.

Acknowledgements This work was supported by a grant from the Hochschulinterne Leistungsförderung (HiLF) of the Hannover Medical School (S.C.H.), and a grant from the Sybille Assmus Stiftung (K.H.T.) For excellent technical assistance, we thank Silke Fischer, Sandra Hagemann, Natascha Heidrich, Nele Korte, Jennifer Metzen, and Hildegard Streich.

Full conflict of interest disclosure is available in the Electronic Supplementary Material for this article.

Conflict of Interest Disclosure No conflicts of interests exist for any of the authors.

References

1. Noble J, Munro CA, Prasad VS, Midha R. Analysis of upper and lower extremity peripheral nerve injuries in a population of patients with multiple injuries. J Trauma 1998;45:116–122.
2. Asplund M, Nilsson M, Jacobsson A, von Holst H. Incidence of traumatic peripheral nerve injuries and amputations in Sweden between 1998 and 2006. Neuroepidemiology 2009;32:217–228.
3. Ciardelli G, Chiono V. Materials for peripheral nerve regeneration. Macromol Biosci 2006;6:13–26.
4. Deumens R, Bozkurt A, Meek MF, et al. Repairing injured peripheral nerves: Bridging the gap. Prog Neurobiol 2010;92:245–276.
5. Lundborg G, Rosen B. Nerve injury and repair — a challenge to the plastic brain. J Peripher Nerv Syst 2003;8:209–226.
6. Brushart TM. Motor axons preferentially reinnervate motor pathways. J Neurosci 1993;13:2730–2738.
7. Uschold T, Robinson GA, Madison RD. Motor neuron regeneration accuracy: Balancing trophic influences between pathways and end-organs. Exp Neurol 2007;205:250–256.
8. Navarro X, Verdu E, Buti M. Comparison of regenerative and reinnervating capabilities of different functional types of nerve fibers. Exp Neurol 1994;129:217–224.
9. Ray WZ, Mackinnon SE. Management of nerve gaps: autografts, allografts, nerve transfers, and end-to-side neurorrhaphy. Exp Neurol 2010;223:77–85.

10. Lundborg G. A 25-year perspective of peripheral nerve surgery: evolving neuroscientific concepts and clinical significance. J Hand Surg [Am] 2000;25:391–414.
11. Mackinnon SE, Hudson AR. Clinical application of peripheral nerve transplantation. Plast Reconstr Surg 1992;90:695–699.
12. Doolabh VB, Hertl MC, Mackinnon SE. The role of conduits in nerve repair: a review. Rev Neurosci 1996;7:47–84.
13. Millesi H. Bridging defects: autologous nerve grafts. Acta Neurochir Suppl 2007;100:37–38.
14. Radtke C, Aizer AA, Agulian SK, Lankford KL, Vogt PM, Kocsis JD. Transplantation of olfactory ensheathing cells enhances peripheral nerve regeneration after microsurgical nerve repair. Brain Res 2009;1254:10–17.
15. Ranvier C, Akiyama Y, Lankford KL, Vogt PM, Krause DS, Kocsis JD. Integration of engrafted Schwann cells into injured peripheral nerve: axonal association and nodal formation on regenerated axons. Neurosci Lett 2005;387:85–89.
16. Levi AD, Guenard V, Aebischer P, Bunge RP. The functional characteristics of Schwann cells cultured from human peripheral nerve after transplantation into a gap within the rat sciatic nerve. J Neurosci 1994;14(3 pt 1):1309–1319.
17. Levi AD, Sonntag VK, Dickman C, et al. The role of cultured Schwann cell grafts in the repair of gaps within the peripheral nervous system of primates. Exp Neurol 1997;143:25–36.
18. Haastert K, Lipokatic E, Fischer M, Timmer M, Grothe C. Differentially promoted peripheral nerve regeneration by grafted Schwann cells over-expressing different FGF-2 isoforms. Neurobiol Dis 2006;21:138–153.
19. Haastert K, Ying Z, Grothe C, Gomez-Pinilla F. The effects of FGF-2 gene therapy combined with voluntary exercise on axonal regeneration across peripheral nerve gaps. Neurosci Lett 2008;443:179–183.
20. Haastert-Talini K, Schaper-Rinkel J, Schmitte R, et al. In vivo evaluation of polysialic acid as part of tissue-engineered nerve transplants. Tissue Eng Part A 2010;16:3085–3098.
21. Haastert-Talini K, Schmitte R, Korte N, Klode D, Ratzka A, Grothe C. Electrical stimulation accelerates axonal and functional peripheral nerve regeneration across long gaps. J Neurotrauma 2011;28:661–674.
22. Lim ST, Airavaara M, Harvey BK. Viral vectors for neurotrophic factor delivery: a gene therapy approach for neurodegenerative diseases of the CNS. Pharmacol Res 2010;61:14–26.
23. Ruff RL, McKerracher L, Selzer ME. Repair and neurorehabilitation strategies for spinal cord injury. Ann N Y Acad Sci 2008;1142:1–20.
24. Boato F, Hendrix S, Huelsenbeck SC, et al. C3 peptide enhances recovery from spinal cord injury by improved regenerative growth of descending fiber tracts. J Cell Sci 2010;123(pt 10):1652–1662.
25. Korte N, Schenk HC, Grothe C, Tipold A, Haastert-Talini K. Evaluation of periodic electrodiagnostic measurements to monitor motor recovery after different peripheral nerve lesions in the rat. Muscle Nerve 2011;44:63–73.
26. Bozkurt A, Tholl S, Wehner S, et al. Evaluation of functional nerve recovery with Visual-SSI--a novel computerized approach for the assessment of the static sciatic index (SSI). J Neurosci Methods 2008;170:117–122.
27. Haastert K, Joswig H, Jaschke KA, Samii M, Grothe C. Nerve repair by end-to-side nerve coaptation: histologic and morphometric evaluation of axonal origin in a rat sciatic nerve model. Neurosurgery 2010;66:567–77.
28. Geuna S, Gigo-Benato D, Rodrigues Ade C. On sampling and sampling errors in histomorphometry of peripheral nerve fibers. Microsurgery 2004;24:72–76.
29. Cheng C, Webber CA, Wang J, et al. Activated RHOA and peripheral axon regeneration. Exp Neurol 2008;212:358–369.
30. Holtje M, Djalali S, Hofmann F, et al. A 29-amino acid fragment of Clostridium botulinum C3 protein enhances neuronal outgrowth, connectivity, and reinnervation. Faseb J 2009;23:1115–1126.
31. Just I, Huelsenbeck SC, Genth H. Clostridium botulinum C3 exoenzyme: rho-inactivating tool in cell biology and a neurotrophic agent. The Open Toxinology Journal 2010;3:19–23.
32. Ahnert-Hilger G, Holtje M, Grosse G, et al. Differential effects of Rho GTPases on axonal and dendritic development in hippocampal neurones. J Neurochem 2004;90:9–18.
33. Hiraga A, Kuwabara S, Doya H, et al. Rho-kinase inhibition enhances axonal regeneration after peripheral nerve injury. J Peripher Nerv Syst 2006;11:217–224.
34. Al-Majed AA, Neumann CM, Brushart TM, Gordon T. Brief electrical stimulation promotes the speed and accuracy of motor axonal regeneration. J Neurosci 2000;20:2602–2608.
35. Lord-Fontaine S, Yang F, Diep Q, et al. Local inhibition of Rho signaling by cell-permeable recombinant protein BA-210 prevents secondary damage and promotes functional recovery following acute spinal cord injury. J Neurotrauma 2008;25:1309–1322.
36. Chen ZW, Wang MS. Effects of nerve growth factor on crushed sciatic nerve regeneration in rats. Microsurgery 1995;16:547–551.
37. Chiu AY, Chen EW, Loera S. A motor neuron-specific epitope and the low-affinity nerve growth factor receptor display reciprocal patterns of expression during development, axotomy, and regeneration. J Comp Neurol 1993;328:351–363.
38. Holtje M, Hoffmann A, Hofmann F, et al. Role of Rho GTPase in astrocyte morphology and migratory response during in vitro wound healing. J Neurochem 2005;95:1237–1248.
39. Holtje M, Hofmann F, Lux R, Veh RW, Just I, Ahnert-Hilger G. Glutamate uptake and release by astrocytes are enhanced by Clostridium botulinum C3 protein. J Biol Chem 2008;283:9289–9299.